Optica Applicata, Vol. LV, No. 2, 2025
DOI: 10.37190/oa/201341

Design of a highly sensitive blood sensor based on a 2D photonic crystal L3 cavity

PUJA SHARMA, SARANG MEDHEKAR*

Department of Physics, Central University of Jharkhand Ranchi, 835222, India

*Corresponding author: sarang.medhekar@cuj.ac.in, smedhekarbit@gmail.com

In this paper, a 2D photonic crystal (PC) biosensor is proposed. The basic PC structure consists of 17×15 holes in X and Z direction over a silicon slab of refractive index (RI) equal to 3.46. The sensor structure consists of two L3 cavities created on the either side of a defect waveguide. The band diagram of the proposed structure is analyzed using plane wave expansion method (PWEM) and simulations of light propagation through the biosensor are carried out using 2D finite difference time domain method (2D-FDTDM). The parameters are optimized to obtain the best possible performance. The sensitivity of the proposed biosensor is determined by the shift in the wavelength of transmission deep as a function of RI of sensing holes. The proposed biosensor exhibits a high-quality factor (Q-factor) of 2587, with a spectral width of 0.6 nm (at the wavelength of 1552 nm) of the transmission deep. The biosensor has ultra-compact footprint of 29 μm^2. Further, it shows a high figure of merit (666 RIU^{-1}), a low detection limit (1.49×10^{-4} RIU), and a maximum sensitivity of 400 nm/RIU. The proposed biosensor might have potential applications in detection of many blood related diseases.

Keywords: photonic crystal (PC), photonic bandgap (PBG), L3 cavity, plane wave expansion method (PWEM), finite difference time domain method (FDTDM).

1. Introduction

Photonic crystals (PCs) are artificially created structures having RI variation in different directions which results in the formation of photonic band gap (PBG). PBG refers to the specific range of optical frequencies at which light propagation is forbidden or restricted within a periodic structure [1,2]. By creating defects such as point and line defects, light can be localized in the defect area [3]. Holes in slab type PCs are mostly preferred for sensing/medical diagnosis application due to ease of fabrication and cost effectiveness [4,5]. Medical diagnosis mainly involves analyzing blood samples to detect various diseases, including communicable and non-communicable ones. The human blood has many constituents like red blood cells (RBC), white blood cells (WBC), platelets, plasma, complex fluid, *etc*. Deficiency of these constituents needs to be treat-

ed to avoid different blood related disorders like thalassemia, lymphoma, nutritional deficiency and leukaemia, *etc*. [6].

Researchers have proposed various innovative designs for optical devices and sensors. MASSOUDI *et al*. [7] produced a PC ring resonator with a super-ellipse shaped core, achieving a transmission efficiency of 95% at $\lambda = 1547.3$ nm, with a bandwidth of 0.7 nm and a quality factor of 2210. The refractive index sensitivity was calculated to be $\Delta\lambda/\Delta n = 0.2$ nm/0.01. RAJASEKAR *et al*. [8] proposed a multicavity coupled photonic crystal ring resonator, realizing a tunable filter with 100% output efficiency, a narrow bandwidth of 0.6 nm, and an ultra-compact footprint of 174.24 μm^2. In contrast, HOSSEINZADEH SANI *et al*. [9] designed a MEMS accelerometer sensor, simulating a resonant peak of 0.8 at 1.644 μm and a quality factor of 3288. Furthermore, RADHOUENE *et al*. [10] developed an add-drop filter that drops a channel at 1636.2 nm, featuring a bandwidth of 0.7 nm, a high quality factor of 2337, and a dropping efficiency of approximately 100%, all within a device size of 412.76 μm^2. Additionally, KRISHNAMOORTHI *et al*. [6] designed and simulated a rhombic-shaped ring resonator biosensor using 2D PC, achieving an average quality factor of 3702, sensitivity of 166 nm/RIU, and transmission efficiency of 80%, and size of 515.29 μm^2. However, these sensors often suffer from limitations such as low sensitivity, narrow detection ranges, large size and complex fabrication processes. In contrast, the proposed 2D PC L3 cavity-based blood sensor offers several distinct advantages. Its optimized design enables high sensitivity, a wide detection range, and a simple fabrication process. Additionally, the sensor's compact size and low power consumption make it an attractive candidate for point-of-care and portable applications. This work aims to leverage these advantages to develop a highly sensitive and practical blood sensor for various biomedical applications.

The current traditional methods of diagnosis in the laboratories is very time consuming and require great human efforts. PCs are label free sensors [11], primarily based on the RI change mechanism. The shift in the resonance wavelength can be seen by infusing various blood samples into the sensing region [4]. It requires minimum time and small quantity of analytes (blood samples) to diagnose a disease [12]. Such sensors are compact, highly sensitive, portable and have low detection limit [13].

Label-free sensors are biosensors that detect biomolecules without relying on fluorescent, radioactive, or enzymatic tags. They work by directly interacting with target molecules, generating a detectable signal. This approach offers several benefits, including simplified assays, increased sensitivity and specificity, real-time monitoring, reduced costs, and versatility in detecting various biomolecules. By eliminating the need for labels, these sensors have the potential to transform biomedical diagnostics and research, as demonstrated by innovative technologies like the 2D PC L3 cavity-based biosensor [14].

Blood testing is a crucial diagnostic tool for detecting various diseases, monitoring health conditions, and tracking treatment efficacy. Conventional blood testing methods, however, often require large sample volumes, complex sample preparation, and expensive equipment [14].

Recent advances in PC technology have enabled the development of highly sensitive and compact biosensors. A 2D PC L3 cavity, in particular, offers a promising platform for blood sensing due to its high quality factor, small mode volume, and ease of fabrication.

This research aims to design a highly sensitive blood sensor based on a 2D PC L3 cavity, capable of detecting minute changes in blood components. The proposed sensor has the potential to revolutionize blood testing by enabling:

1) Fast and accurate detection of biomarkers and analytes.
2) Minimal sample volume requirements.
3) Low-cost and compact device design.
4) Point-of-care testing capabilities.

By developing a highly sensitive blood sensor based on a 2D PC L3 cavity, this research seeks to make a significant impact in the field of biomedical diagnostics and improve healthcare outcomes.

In light of the above mentioned, a PC biosensor is proposed here. The sensitivity of the proposed biosensor is determined by the shift in the wavelength of transmission deep as a function of RI of sensing holes [14]. The proposed biosensor exhibits high-quality factor (Q-factor) of 2587, with a spectral width of 0.6nm of the transmission deep (at the wavelength of 1552 nm). The proposed biosensor shows a high figure of merit (666 RIU^{-1}), a low detection limit (1.49×10^{-4} RIU), and a maximum sensitivity of 400 nm/RIU. The biosensor has ultra-compact footprint of 29 μm^2. The proposed biosensor can be used to detect many blood related disorders like thalassemia, leukaemia, lymphoma and nutritional deficiency, *etc*.

2. Design and band diagram of the proposed biosensor

As shown in Fig. 1, the proposed biosensor is designed on a 2D hexagonal lattice PC comprising of 17×15 air holes in *X*- and *Z*-direction over silicon slab. The parameters are optimized to obtain the best possible performance which are lattice constant (a = 339 nm), radius of holes ($r = 0.295a$), RI of holes (n = 1), and RI of the slab (n_1 = 3.46). The sensor structure consists of two L3 cavities created on the either side

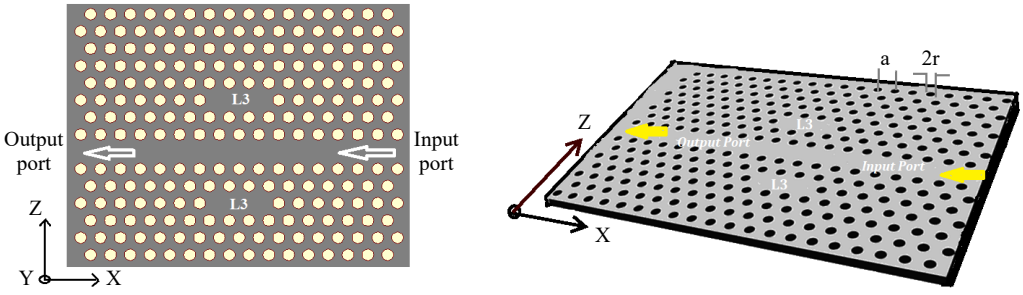

Fig. 1. Schematic of proposed biosensor.

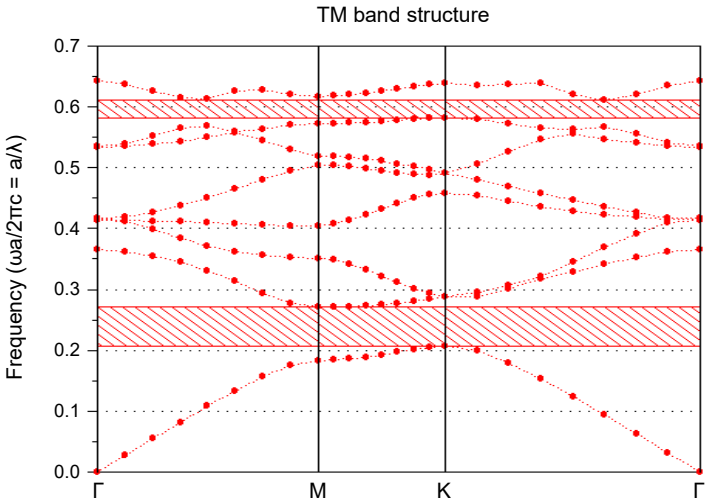

Fig. 2. Band structure of the proposed structure for TM polarization.

of one defect waveguide. Band diagram of proposed structure has been calculated using PWEM for transverse magnetic (TM) polarization which is shown in Fig. 2. It has two PBG of normalized wavelength ranging from $0.21 < a/\lambda < 0.28$ and $0.57 < a/\lambda < 0.61$. Design parameters of the proposed blood sensor are listed in Table 1.

T a b l e 1. Design parameters of proposed blood sensor

Parameter	Specification
Configuration	Holes in slab
Rod shape	Circular
Lattice structure	Triangular
Lattice constant a	339 nm
Radius of the air holes r	$0.295a$
RI of the Si slab	3.46
PBG	$0.21 < a/\lambda < 0.28$ and $0.57 < a/\lambda < 0.61$
Height of slab	$0.7a$
Number of rods in X- and Z-directions	17×15
Footprint	29 μm^2

3. Numerical investigations and results

Simulation-based investigations of the proposed biosensor are performed using 2D-FDTDM that solves Maxwell's equation in time domain [15]. Grid size is chosen to be $a/16$ in X- and Z-directions. Perfectly matched layer (PML) is used to avoid back reflections from boundaries of simulation domain [16]. Fullwave module (based on

FDTD technique) by Synopsys group is used for the investigations. The computer configuration consists of a 3.10 GHz processor, a 64-bit operating system, and 20 GB of RAM. The time step of $\Delta t = 0.01490$ s was used in the FDTD simulation, providing stable output.

A wide spectral optical input is launched at the input port and normalized transmission spectrum is obtained at the output port. At the wavelength of 1552 nm, the input signal is completely suppressed at the output port. While the wavelength other than 1552 nm, it shows high transmission. Hence, a dip is detected at the output spectrum as shown in Fig. 3. The magnetic field distributions within the proposed structure are obtained for 1550 and for 1552 nm (wavelength of the transmission deep) as shown in Fig. 4(a) and (b), respectively.

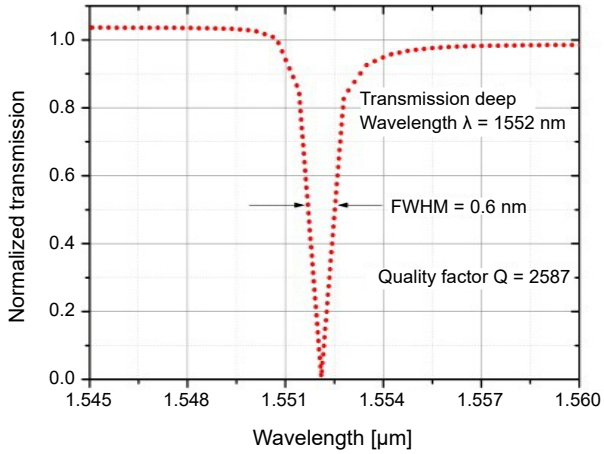

Fig. 3. Normalized transmission at the output port.

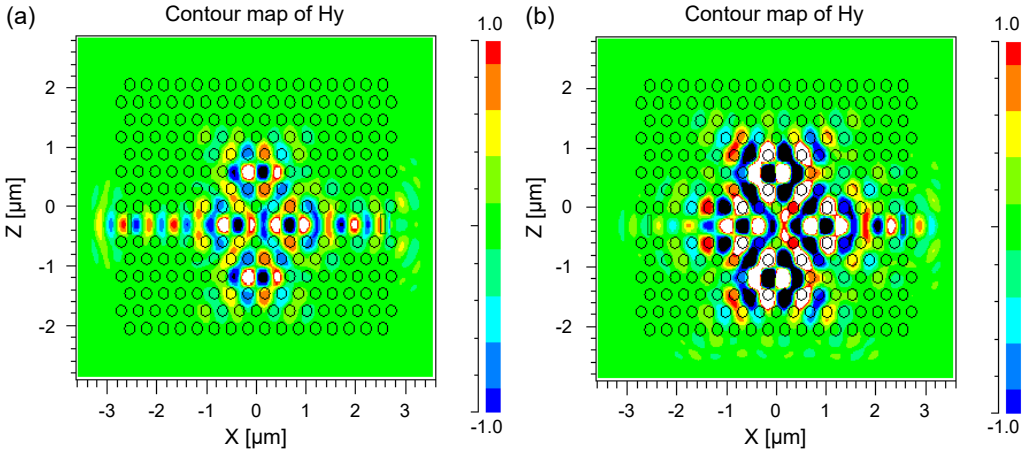

Fig. 4. Magnetic field distribution for (a) wavelength of 1550 nm, and (b) transmission deep wavelength of 1552 nm.

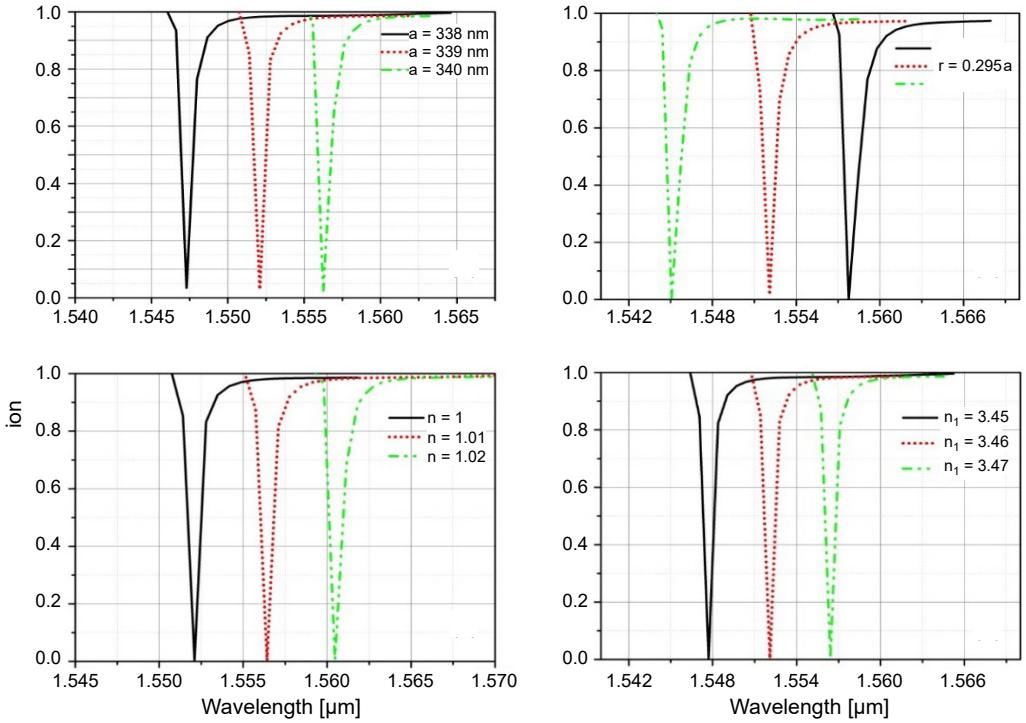

Fig. 5. Varied (a) lattice constant a, (b) radius of holes r, (c) RI of holes n, and (d) RI of the slab n_1 for the best possible performance of the sensor.

Lattice constant a, radius of holes r, RI of holes n, and RI of the slab n_1 are varied to obtain the best possible performance as shown in Figs. 5(a)–(d), respectively. The optimized parameters are lattice constant (a = 339 nm), radius of holes ($r = 0.295a$), RI of holes (n = 1), and RI of the slab (n_1 = 3.46). These parameters are likely considered optimal due to a combination of factors that enhance the performance of the 2D PC L3 cavity-based blood sensor.

4. Biosensor

The proposed coupled L3 cavities-based biosensor can detect diverse range of blood constituents. The normalized spectrum comparing nine different blood components is as shown in Fig. 6. The sensitivity of the proposed biosensor is determined by the shift in the wavelength of transmission deep as a function of RI of sensing holes. Further, as shown in Fig. 7, the wavelength shifts linearly as the holes refractive index changes which are highly desirable. The sensors performance is evaluated in the presence of blood components listed in Table 2.

In PC slab sensors, it is often more practical to separate blood components before testing, rather than introducing whole blood into the sensor. This is because whole blood can clog the sensor's nanostructured features and affect its performance [17].

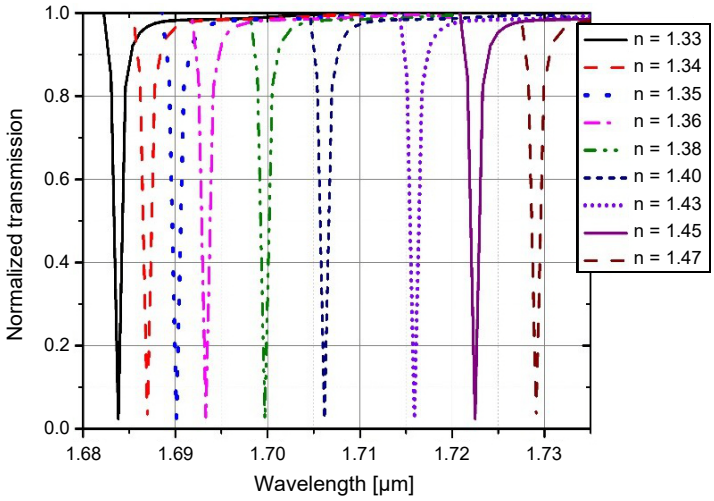

Fig. 6. Normalized output spectrum for different blood components.

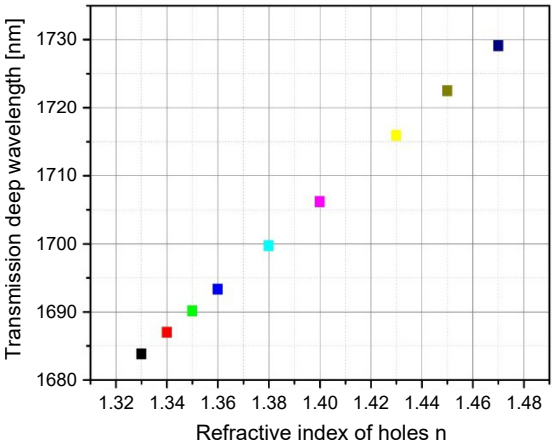

Fig. 7. Shifts in the transmission deep wavelength as a result of variations in the refractive indices of a variety of blood compoents.

Separating blood components, such as plasma or serum, can help to improve the sensor's accuracy and reliability [18,19]. The required sample volume is typically on the order of picoliters (pL) to femtoliters (fL). According to [20], the sample volume required is approximately 6.35 μg/mL to 1.27 mg/mL. Another study published a sample volume of around 10 μg/mL [17].

The power requirements of the PC-based sensor are an essential consideration for its practical implementation. The power consumption of a PC-based structure can be as low as 210 nW at 1.5 μm [21].

The 2D PC L3 cavity-based biosensor operates on the principle of refractive-index -based detection. When light is incident on the PC structure, it interacts with the peri-

T a b l e 2. Performance of the biosensor.

Hole-filling substance	Refractive index n	Transmission deep wavelength λ [nm]
Water	1.33	1683.81
Cytop	1.34	1686.97
Blood plasma	1.35	1690.14
WBC	1.36	1693.32
Hemoglobin	1.38	1699.71
RBC	1.40	1706.16
Sylgard184	1.43	1715.91
Biotin-Streptavidin	1.45	1722.48

odic arrangement of air holes, resulting in the formation of a PBG. The PBG is a range of frequencies where light is forbidden to propagate through the structure. The L3 cavity, formed by removing three air holes on both sides of waveguide of the PC structure, creates a localized defect mode within the PBG. This cavity mode is highly sensitive to changes in the refractive index of the surrounding medium. When a blood component with an unknown refractive index is introduced into the sensor, it alters the refractive index of the surrounding medium. This change in refractive index shifts the cavity mode resonance wavelength, which can be measured using spectroscopic techniques. The sensitivity of the sensor is enhanced by the high quality factor (Q-factor) of the L3 cavity, which amplifies the interaction between the light and the blood component. Additionally, the small mode volume of the cavity mode further increases the sensitivity of the sensor.

The sensing mechanism of the 2D PC L3 cavity-based biosensor can be summarized as follows:

1) PBG formation due to the periodic arrangement of air holes.
2) Cavity mode formation within the PBG due to the L3 cavity.
3) Refractive index sensing through the shift in cavity mode resonance wavelength.
4) Sensitivity enhancement due to the high Q-factor and small mode volume of the cavity mode.

Due to the complexity and scope of these derivations, detailed mathematical expressions and calculations are not included in this manuscript. However, the interested reader is referred to [22] for a comprehensive treatment of the underlying mathematics.

The L3 cavity is a type of PC cavity that consists of three missing holes in a triangular lattice of air holes in a silicon slab [23] is specific cavity design creates a highly localized and confined optical mode, which enhances the interaction between the light and the surrounding medium [24]. Table 3 shows the concise comparison of the L3 cavity with other common cavity types mentioned in [24-27]. Table 4 shows the different formula used to detect the calculated parameters.

T a b l e 3. A concise comparison of the L3 cavity with other common cavity types [24-27].

Cavity type	Number of missing holes	Mode volume	Q-factor	Advantages
L1	1	Large	Low	Simple fabrication, low sensitivity
L2	2	Medium	Medium	Balanced sensitivity and Q-factor
L3	3	Small	High	High sensitivity, high Q-factor, suitable for biosensing
H1	1	Large	Low	Simple fabrication, low sensitivity
H3	3	Small	High	High sensitivity, high Q-factor, but more challenging fabrication

T a b l e 4. The basic formula used for the biosensor.

Quantity	Formula	Terms used
Transmission	$T = P_{out}/P_{in}$	P_{out} – power output P_{in} – power input
Quality factor	$Q = \lambda/\text{FWHM}$	λ – off-resonance wavelength FWHM – full width at half maximum
Sensitivity	$S = \Delta\lambda/\Delta n$	$\Delta\lambda$ – shift in transmission deep wavelength Δn – change in refractive index of holes
Figure of merit	$\text{FOM} = S/\text{FWHM}$	
Detection limit	$\text{DL} = \lambda/(10QS)$	Q – quality factor S – RI sensitivity
Size	$17a \times 15a$	a – lattice constant

The L3 cavity offers a unique combination of high sensitivity, high Q-factor, and relatively simple fabrication, making it an attractive choice for biosensing applications [28].

The use of a heterostructure cavity instead of the L3-L3 cavity configuration could have significant implications for PC cavity design. According to [29], heterostructure cavities offer improved optical performance, including higher quality factors and smaller mode volumes, compared to traditional L3-L3 cavities. However, they also present additional design and fabrication challenges, such as the need for precise control over layer thicknesses and interface roughness [30].

Overall, the choice between a heterostructure cavity and an L3-L3 cavity configuration will depend on the specific requirements of the application, including the desired optical performance, design complexity, and fabrication feasibility.

Table 5 presents a comparison of the proposed blood sensor with other PC designs. To provide a more comprehensive comparison, we extend this comparison to include non-PC-based sensors. The proposed blood sensor shows considerable performance enhancement as compared to previous designs. The proposed PC sensor offers high sensitivity, compact size, and low power consumption, making it suitable for point-of-care

T a b l e 5. Comparison of the proposed blood sensor with various PCs designs.

Reference	Year	Q-factor	Sensitivity [nm/RIU]	Figure of merit [RIU^{-1}]	Detection limit [RIU]	Footprint [μm^2]
[7]	2019	2210	–	–	–	383.89
[8]	2019	2583.50	–	–	–	174.24
[9]	2021	3288	–	0.97	–	104.35
[10]	2021	2337	–	–	–	412.76
[31]	2022	5166	1.87–2.94	9.84	0.021	–
[32]	2022	–	161 deg/RIU	67.93	0.4219 deg^{-1}	–
[6]	2023	3702	166	392.5	1.4×10^{-4}	515.29
[33]	2025	173.46	432.06	–	0.7459	–
Present study	2025	2587	400	666	1.49×10^{-4}	29

applications. However, it has a limited detection range and requires sophisticated fabrication techniques.

5. Conclusions

A label-free biosensor based on 2D PC coupled L3 cavities created by periodic holes in silicon slab is described in this paper. The biosensor shows transmission deep at the wavelength of 1552 nm exhibits high-quality factor (2587) and narrow spectral width (0.6 nm). The proposed sensor shows a high figure of merit (666 RIU^{-1}) and a low detection limit (1.49×10^{-4} RIU). The sensor exhibits a maximum sensitivity of 400 nm/RIU. The proposed biosensor can be used to detect many blood related disorders like thalassemia, leukaemia, lymphoma and nutritional deficiency, *etc*.

References

[1] SHARMA P., MEDHEKAR S., *Frequency comb generation in rod type 2D photonic crystal coupled cavity waveguide*, Journal of Optics **53**, 2023: 590-595. https://doi.org/10.1007/s12596-023-01218-6

[2] SHARMA P., GUPTA M.M., GHOSH N., MEDHEKAR S., *2D photonic crystal based all-optical add-drop filter consisting of square ring resonator*, Materials Today: Proceedings, Vol. 66, Part 7, 2022: 3344 -3348. https://doi.org/10.1016/j.matpr.2022.07.062

[3] JOANNOPOULOS J.D., JOHNSON S.G., WINN J.N., MEADE R.D., *Photonic Crystals: Molding the Flow of Light*, 2011.

[4] SHARMA P., MEDHEKAR S., *Ring resonator-based highly sensitive chemical/biochemical sensor created on holes in silicon slab 2D photonic crystal*, Journal of Optics **52**, 2023: 2315-2322. https://doi.org/10.1007/s12596-023-01149-2

[5] SHARMA P., GHOSH N., GUPTA M.M., MEDHEKAR S., *Add-drop filter and refractive index and temperature sensor using 2D photonic crystal ring resonator*, International Journal of Optics and Photonics (IJOP) **16**(2), 2022: 221-232. https://doi.org/10.52547/ijop.16.2.221

[6] KRISHNAMOORTHI B., CAROLINE ELIZABETH B., MICHAEL M., THIRUMARAN S., *A novel rhombic shaped photonic crystal bio-sensor for identifying disorders in the blood samples*, Optical and Quantum Electronics **55**, 2023: 312. https://doi.org/10.1007/s11082-023-04584-4

[7] Massoudi R., Najjar M., Mehdizadeh F., Janyani V., *Investigation of resonant mode sensitivity in PhC based ring resonators*, Optical and Quantum Electronics **51**, 2019: 87. https://doi.org/10.1007/s11082-019-1793-0

[8] Rajasekar R., Jayabarathan J.K., Robinson S., *Nano-optical filter based on multicavity coupled photonic crystal ring resonator*, Physica E: Low-dimensional Systems and Nanostructures **114**, 2019: 113591. https://doi.org/10.1016/j.physe.2019.113591

[9] Hosseinzadeh Sani M., Saghaei H., Mehranpour M.A., Tabrizi A.A., *A novel all-optical sensor design based on a tunable resonant nanocavity in photonic crystal microstructure applicable in MEMS accelerometers*, Photonic Sensors **11**, 2021: 457-471. https://doi.org/10.1007/s13320-020-0607-0

[10] Radhouene M., Balaji V.R., Najjar M., Robinson S., Janyani V., Murugan M., *Rounded square ring resonator based add drop filter for WDM applications using two dimensional photonic crystals*, Optical and Quantum Electronics **53**, 2021: 273. https://doi.org/10.1007/s11082-021-02924-w

[11] Sharma P., Medhekar S., *"Fluid nonlinear coefficient sensor" designed on 2D photonic crystal*, Journal of Optics **53**, 2024: 4616-4622. https://doi.org/10.1007/s12596-023-01617-9

[12] Olyaee S., Mohebzadeh-Bahabady A., *Designing a novel photonic crystal nano-ring resonator for biosensor application*, Optical and Quantum Electronics **47**, 2015: 1881-1888. https://doi.org/10.1007/s11082-014-0053-6

[13] Sharma P., Medhekar S., *Ultra-compact photonic crystal nanocavity-based sensor for simultaneous detection of refractive index and temperature*, Journal of Optics **52**, 2023: 504-509. https://doi.org/10.1007/s12596-022-01037-1

[14] Lifson M.A., Ozen M.O., Inci F., Wang S.Q., Inan H., Baday M., Henrich T.J., Demirci U., *Advances in biosensing strategies for HIV-1 detection, diagnosis, and therapeutic monitoring*, Advanced Drug Delivery Reviews **103**, 2016: 90-104. https://doi.org/10.1016/j.addr.2016.05.018

[15] López-Alonso J. M., Rico-García J. M., Alda J., *Photonic crystal characterization by FDTD and principal component analysis*, Optics Express **12**(10), 2004: 2176-2186. https://doi.org/10.1364/opex.12.002176

[16] Shi S., Chen C., Prather D.W., *Plane-wave expansion method for calculating band structure of photonic crystal slabs with perfectly matched layers*, Journal of the optical society of America A **21**(9), 2004: 1769-1775. https://doi.org/10.1364/JOSAA.21.001769

[17] Threm D., Nazirizadeh Y., Gerken M., *Photonic crystal biosensors towards on-chip integration*, Journal of Biophotonics **5**(8-9), 2012: 601-616. https://doi.org/10.1002/jbio.201200039

[18] Lifson M.A., Miller B.L., *Photonic crystals as robust label-free biosensors*, [In] Serpe M.J., Kang Y., Zhang Q.M. [Eds.], *Photonic Materials for Sensing, Biosensing and Display Devices*, Springer Series in Materials Science, Vol. 229, Springer, Cham, 2016. https://doi.org/10.1007/978-3-319-24990-2_7

[19] Liang L., Xie F., Jin L., Yang B., Sun L.P., Guan B.O., *Optical microfiber biomedical sensors: Classification, applications, and future perspectives*, Advanced Sensor Research **4**(5), 2025: 2400185. https://doi.org/10.1002/adsr.202400185

[20] Inan H., Poyraz M., Inci F., Lifson M.A., Baday M., Cunningham B.T., Demirci U., *Photonic crystals: emerging biosensors and their promise for point-of-care applications*, Chemical Society Reviews **46**(2), 2017: 366-388. https://doi.org/10.1039/C6CS00206D

[21] Jang H., Karnadi I., Pramudita P., Song J.H., Soo Kim K., Lee Y.H., *Sub-microWatt threshold nanoisland lasers*, Nature Communications **6**, 2015: 8276. https://doi.org/10.1038/ncomms9276

[22] Bogaerts W., De Heyn P., Van Vaerenbergh T., De Vos K., Kumar Selvaraja S., Claes T., Dumon P., Bienstman P., Van Thourhout D., Baets R., *Silicon microring resonators*, Laser and Photonics Reviews **6**(1), 2012: 47-73. https://doi.org/10.1002/lpor.201100017

[23] Akahane Y., Asano T., Song B.-S., Noda, S., *High-Q photonic nanocavity in a two-dimensional photonic crystal*, Nature **425**, 2003: 944-947. https://doi.org/10.1038/nature02063

[24] Zhang Y.N., Zhao Y., Lv R.Q., *A review for optical sensors based on photonic crystal cavities*, Sensors and Actuators A: Physical **233**, 2015: 374-389. https://doi.org/10.1016/j.sna.2015.07.025

[25] WANG F., SIGMUND O., *Optimization of photonic crystal cavities*, 2017 International Conference on Numerical Simulation of Optoelectronic Devices (NUSOD), Copenhagen, Denmark, 2017: 39-40. https://doi.org/10.1109/NUSOD.2017.8009980

[26] SALDUTTI M., XIONG M., DIMOPOULOS E., YU Y., GIOANNINI M., MØRK J., *Modal properties of photonic crystal cavities and applications to lasers*, Nanomaterials **11**(11), 2021: 3030. https://doi.org/10.3390/nano11113030

[27] BENMERKHI A., BOUCHEMAT M., BOUCHEMAT T., *Ultrahigh-Q of the L3 photonic crystal microcavity*, Optik **124**(22), 2013: 5719-5722. https://doi.org/10.1016/j.ijleo.2013.04.028

[28] KURAMOCHI E., TANIYAMA H., TANABE T., SHINYA A., NOTOMI M., *Ultrahigh-Q two-dimensional photonic crystal slab nanocavities in very thin barriers*, Applied Physics Letters **93**(11), 2008: 111112. https://doi.org/10.1063/1.2987459

[29] SONG B.S., NODA S., ASANO T., AKAHANE Y., *Ultra-high-Q photonic double-heterostructure nanocavity*, Nature Materials **4**, 2005: 207-210. https://doi.org/10.1038/nmat1320

[30] SHI P., *High-Q photonic crystal heterostructure microcavities by tuning air holes*, Optics Communications **446**, 2019: 88-92. https://doi.org/10.1016/j.optcom.2019.04.072

[31] PARANDIN F., HEIDARI F., ASLINEZHAD M., PARANDIN M. M., ROSHANI S., ROSHANI S., *Design of 2D photonic crystal biosensor to detect blood components*, Optical and Quantum Electronics **54**, 2022: 618. https://doi.org/10.1007/s11082-022-03945-9

[32] KARKI B., VASUDEVAN B., UNIYAL A., PAL A., SRIVASTAVA V., *Hemoglobin detection in blood samples using a graphene-based surface plasmon resonance biosensor*, Optik **270**, 2022: 169947. https://doi.org/10.1016/j.ijleo.2022.169947

[33] ANGADALA S., CHEERLA S., MALAKALAPALLI S., VASIMALLA Y., BEN KHALIFA S., CHEBAANE S., *A label -free surface plasmon resonance biosensor for chemical sensing*, Plasmonics, 2025. https://doi.org/10.1007/s11468-025-03168-0

Received October 27, 2024
in revised form January 5, 2025